Optimal design of short-period structures equipped with Sliding Tuned Liquid Column Damper and numerical and experimental control performance evaluation

Chiara Masnata[1*], Christoph Adam[2] and Antonina Pirrotta[1]

[1]University of Palermo, Department of Engineering, Viale delle Scienze, 90128 Palermo, Italy
[2]Unit of Applied Mechanics, University of Innsbruck, Technikerstr. 13, Innsbruck, Austria

*chiara.masnata@unipa.it

Abstract. In this paper, the structural vibration control of short-period systems by a sliding model of a Tuned Liquid Column Damper (herein referred to as STLCD) is investigated from both theoretical and experimental points of view. The proposed STLCD is essentially composed of a U-tube container with liquid inside, which can slide on a linear guide rail and is connected to the structure by a spring-dashpot system. Unlike traditional fixed TLCDs, this type of arrangement allows the proposed STLCD to be tuned to short-period structural systems since the spring can be used for tuning while the dashpot provides additional damping. Details on the selection of the optimal design parameters of the STLCD are provided and the validity of the introduced mathematical model is verified both in time and frequency domains through experimental tests conducted at the Laboratory of Experimental Dynamics at the University of Palermo, Italy. For the experimental tests, a scale model of an STLCD-controlled structure is considered, focusing on the reduction of the roof accelerations. Finally, for comparison purposes, the control performance of the proposed control strategy for the vibration suppression of stiff structures is evaluated by analyzing its structural responses in contrast to the corresponding uncontrolled structure under harmonic excitations.

Keywords: vibration control; sliding tuned liquid column damper; experimental study; small-scale experiments.

1 Introduction

In the field of structural control, Tuned Liquid Column Dampers (TLCDs) have received considerable attention as prominent passive control mechanisms for mitigating vibrations induced by dynamic excitations such as wind and earthquakes [1,2]. TLCDs are basically U-shaped containers, filled with liquid to a proper level and attached to the system to be controlled. Structural vibration suppression is achieved by the movement of the liquid and the hydrodynamic head losses that occur as the liquid moves within the TLCD [3]. Additionally, for increased dissipation requirements, openings or embossments can be inserted in the channels of the TLCD [4,5]. In this regard, the influence of different inner orifice opening ratios and TLCD dimensions on the control efficacy has been experimentally investigated in [6,7].

Due to the inherent long-period nature of TLCDs, early investigations focused mainly on the application of these devices in flexible structures such as tall and slender structures, which are characterized by high natural periods and are highly prone to wind-induced vibrations [8,9]. In these studies, TLCDs were found to be attractive devices because of some of their particular characteristics, such as low cost, easy installation, lack of required maintenance, and no need to add solid mass to the main structure. Therefore, subsequent analyses started to consider the use of TLCDs for vibration control of structures subjected to seismic forces [10]. From the previous investigations, it can be seen that the efficiency of a TLCD depends on the precise tuning and the correct choice of damping. Thus, the optimal design of the TLCD is crucial for reducing the structural response. Generally, the optimal design of this device is approached through numerical procedures in order to accurately account for the

real characteristics of the primary system. In [11], optimal design parameters of the TLCD for mitigating the wind-induced response of a 76-story benchmark building were obtained numerically. However, the structural damping and nonlinear behavior that characterizes the TLCD make it difficult to perform numerical analyses and evaluate the optimal parameters. In particular, numerical procedures are not suitable for the preliminary design stage, which requires a quick estimation of the TLCD parameters. To address this challenge, many studies have proposed simplified approaches [12]. For instance, explicit design formulas for TLCD parameters have been derived by assuming undamped primary structures under harmonic vibrations [13]. Similarly, in [14], useful design formulas for TLCD were obtained in closed form for undamped primary structures under broad-band white noise excitation of either wind or earthquake-type loads.

In this context, direct approaches could be developed by resorting to the use of equivalent linearization techniques. In this way, the analytical formulas for evaluating the TLCD parameters and for predicting the behavior of a damped main system under random loads were provided [15,16]. Moreover, the successful application of direct approaches and the significant control performance of the TLCD for reducing the structural responses of flexible structures led to extend its use to base-isolated structures, which are also characterized by elongated periods as well [17]. In this context, the straightforward procedure proposed previously in [15] for the optimal design of the TLCD for the vibration control of fixed-base structures has been extended to the case of base-isolated structures in order to mitigate the displacements at the isolation floor [18]. Furthermore, experimental tests conducted on small-scale models of a single-degree-of-freedom (SDOF) base-isolated structure subjected to a base excitation proved the TLCD efficacy [19,20]. From the majority of the previous studies, it can be seen that most of the existing research on TLCDs as seismic vibration control devices has predominantly focused on flexible structures.

However, seismic excitations encompass a broader frequency bandwidth, rich in high-frequency content compared to wind-induced vibrations, which can be potentially hazardous to both flexible and stiff structures. Tuning the TLCD to match the shorter periods of such structures presents challenges in achieving feasible lengths of the TLCD column tube. The need to tune the TLCD frequency to match the frequency of the structure further limits its application to stiffer structural configurations.

Consequently, efforts have been made to extend their utility to short-period structures, leading to the conceptualization of a translational spring-connected model of TLCD, herein referred to as Sliding TLCD (STLCD). As can be seen in Fig. 1, the STLCD essentially consists of a conventional TLCD that can slide along a linear guide rail and is connected to the structure via a spring-dashpot system. This flexible mounting mechanism expands the range of structural systems to which the STLCD can be tailored. [21]. However, it should be emphasized that the optimal design of the STLCD presents difficulties analogous to those of the TLCD since this device is also governed by nonlinear equations of motion. In previous studies, characteristic parameters of the STLCD were only numerically optimized with the aim of minimizing the displacement response of the structure. It should be emphasized that these procedures can be computationally demanding in a design phase, resulting in parameters that are not easily applicable in real design processes. Moreover, the existing literature has mainly studied this configuration from a theoretical point of view.

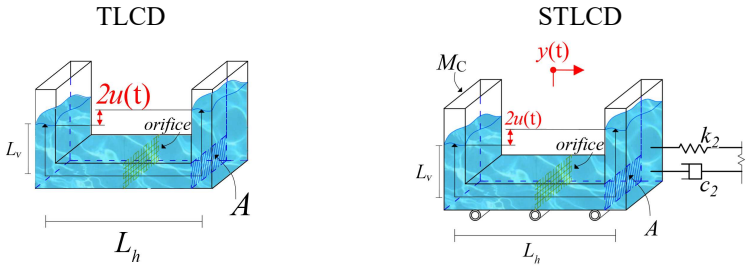

Fig.1 Schematic structure of (a) TLCD device; (b) STLCD device

Therefore, in the present paper, this innovative STLCD configuration is theoretically and experimentally investigated to provide a closed-form formula of the optimal STLCD parameters for the vibration control of short-period structures. As a first novel contribution of this study, the proposed STLCD optimization procedure, unlike the optimization techniques developed in [21], seeks those parameters that minimize the seismic response of the SDOF structure in terms of top-story accelerations. Moreover, approximate closed-form formulas of the STLCD parameters are obtained by taking into account a statistical linearization technique and by assuming a white noise

process as base excitations, without resorting to unwieldy numerical algorithms. Finally, the reliability of the proposed formulation and the dynamic behavior of the STLCD are explored for the first time in both time and frequency domains through experimental studies. Shake table tests have been performed at the Laboratory of Experimental Dynamics, University of Palermo, Italy, employing a small-scale model of the STLCD-controlled structure. Furthermore, for comparison, the efficiency of the proposed control strategy in suppressing vibrations in stiff structures was assessed by analyzing the structural responses in contrast to the uncontrolled counterpart, under harmonic excitations, with particular emphasis on the reduction of roof accelerations.

2 Mathematical formulation

Consider the planar model of the STLCD-controlled structure (Fig.2), subjected to the base acceleration $\ddot{x}_g(t)$. Let $x_s(t)$ denote the horizontal displacement of the main system relative to the ground and M_s, C_s and K_s its mass, damping, and stiffness coefficients, respectively. As depicted in Fig.2, the STLCD device comprises a U-shaped container, partially filled with liquid, linked to the primary system via a spring with stiffness k_2 and a damper with damper coefficient c_2. The vertical displacement of the liquid and the lateral movement of the container are denoted as $u(t)$ and $y(t)$, respectively. The container has a mass equal to M_c and a constant cross-sectional area A. Additionally, L_v and L_h represent the liquid height in one of the two vertical columns in static conditions and the horizontal length of the device, respectively, thus, the total length of the liquid can be expressed as $L = L_h + 2L_v$. The liquid mass is $m_l = \rho AL$, where ρ stands for the liquid density, commonly water. As mentioned above, orifices can be installed in the container to increase the damping effect due to the head losses caused by the fluid passing through them. In this study, the simple configuration without orifices is considered.

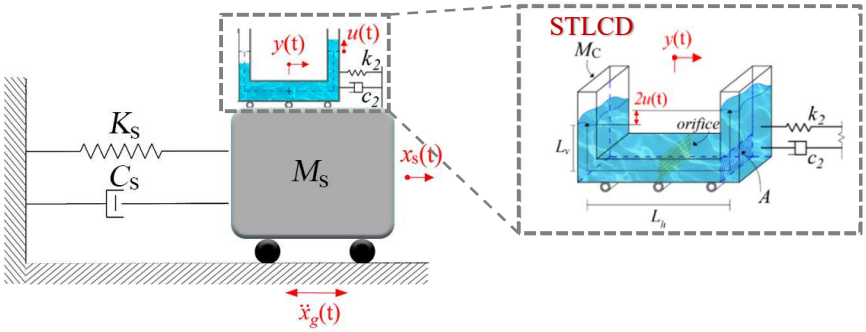

Fig.2 Proposed STLCD-controlled structure

The governing equations of motion of the STLCD-controlled structure, excited at the base, are [21]:

$$
\begin{aligned}
&M_s\ddot{x}_s(t)+C_s\dot{x}_s(t)+K_s x_s(t)-c_2\dot{y}(t)-k_2 y(t)=-M_s\ddot{x}_g(t)\\
&(\rho AL+M_c)\ddot{x}_s(t)+(\rho AL+M_c)\ddot{y}(t)+\rho AL_h\ddot{u}(t)+c_2\dot{y}(t)+k_2 y(t)=-(\rho AL+M_c)\ddot{x}_g(t)\\
&\rho AL_h\ddot{x}_s(t)+\rho AL_h\ddot{y}(t)+\rho AL\ddot{u}(t)+\frac{\rho A}{2}\xi|\dot{u}(t)|\dot{u}(t)+2\rho Agu(t)=-\rho AL_h\ddot{x}_g(t)
\end{aligned}
\tag{1}
$$

where g is the acceleration of gravity and ξ is the head loss coefficient, introduced to model the hydrodynamic head losses experienced as the liquid moves inside the vessel [4,15]. Using the substitution $-c_2\dot{y}(t)-k_2 y(t)=(\rho AL+M_c)\ddot{x}_s(t)+(\rho AL+M_c)\ddot{y}(t)+\rho AL_h\ddot{u}(t)+(\rho AL+M_c)\ddot{x}_g(t)$ in the first equation, and normalizing with respect to M_s, $\rho AL+M_c$, ρAL, Eq. (1) can be written in a more convenient form as

$$\begin{cases}(1+\mu_t)\ddot{x}_s(t)+\mu_t\ddot{y}(t)+\alpha\mu_l\ddot{u}(t)+2\zeta_s\omega_s\dot{x}_s(t)+\omega_s^2 x_s(t)=-(1+\mu_t)\ddot{x}_g(t)\\ \ddot{x}_s(t)+\ddot{y}(t)+\alpha\mu_l\ddot{u}(t)/\mu_t+2\zeta_2\omega_2\dot{y}(t)+\omega_2^2 y(t)=-\ddot{x}_g(t)\\ \alpha\ddot{x}_s(t)+\alpha\ddot{y}(t)+\ddot{u}(t)+\xi|\dot{u}(t)|\dot{u}(t)/(2L)+\omega_l^2 u(t)=-\alpha\ddot{x}_g(t)\end{cases} \quad (2)$$

In Eq. (2), $\alpha = L_h / L$ denotes the length ratio and $\mu_t = \mu_l + \delta$ is the total mass ratio of the STLCD, which includes both the liquid mass ratio $\mu_l = \rho AL / M_s$ and the container mass ratio $\delta = M_c / M_s$. Furthermore, $\omega_l = \sqrt{2g/L}$ is the natural frequency of the liquid, while $\omega_2 = \sqrt{k_2/(\rho AL + M_c)}$ and $\zeta_2 = c_2/\left[2\omega_2(\rho AL + M_c)\right]$ are the natural frequency and the damping ratio of the STLCD container, respectively. Note that by preventing the STLCD from moving ($y(t)=0$), the system of equations governing the response of the main structure excited at its base and equipped with a standard TLCD is retrieved.

Similar to TLCDs, as shown in Eqs. (1)-(2), the STLCD also exhibits slightly nonlinear behavior, and equivalent mechanical models may be employed to streamline the analyses required for the optimal design of the device [15,16]. In the following sections, the reliability of adopting an equivalent linear model is discussed through numerical and experimental investigations.

2.1 Statistical linearization technique

The nonlinear formulation of the STLCD-controlled structure presented in Eq. (2) can be linearized by applying techniques such as the Statistical Linearization Technique (SLT) [22]. In this context, the main system equipped with an STLCD is assumed to be subjected to a random excitation modeled as a zero-mean Gaussian white noise process. It follows that the dynamic responses of both the primary system and the device, as well as their derivatives, are also stochastic processes (denoted by capital letters, as is customary) [15]. Therefore, by applying the SLT, the original nonlinear system Eq. (2) can be replaced by an equivalent linear system as

$$\begin{aligned}&(1+\mu_t)\ddot{X}_s(t)+\mu_t\ddot{Y}(t)+\alpha\mu_l\ddot{U}(t)+2\omega_s\zeta_s\dot{X}_s(t)+\omega_s^2 X_s(t)=-(1+\mu_t)\ddot{X}_g(t)\\ &\ddot{X}_s(t)+\ddot{Y}(t)+\alpha\mu_l\ddot{U}(t)/\mu_t+2\omega_2\zeta_2\dot{Y}(t)+\omega_2^2 Y(t)=-\ddot{X}_g(t)\\ &\alpha\ddot{X}_s(t)+\alpha\ddot{Y}(t)+\ddot{U}(t)+2\omega_l\zeta_l\dot{U}(t)+\omega_l^2 U(t)=-\alpha\ddot{X}_g(t)\end{aligned} \quad (3)$$

where the term $\xi|\dot{U}(t)|\dot{U}(t)/(2L)$ has been replaced by $2\zeta_l\omega_l\dot{U}(t)$ in the last equation and the equivalent damping ratio ζ_l has been introduced. The error between the nonlinear system in Eq. (2) and its corresponding linear counterpart in Eq. (3) is

$$\varepsilon = \frac{1}{2L}\xi|\dot{U}(t)|\dot{U}(t) - 2\omega_l\zeta_l\dot{U}(t) \quad (4)$$

Hence, the value of the equivalent damping ratio ζ_l is given by minimizing the mean square of the error with respect to ζ_l [15]. Specifically, according to the analysis presented in [15], the expression for the equivalent damping ratio is

$$\zeta_l = \frac{\xi}{2L\,\omega_l}\sqrt{\frac{2}{\pi}}\sigma_{\dot{U}} \quad (5)$$

As can be seen from Eq. (5), ζ_l depends on the response $\sigma_{\dot{U}}$, which represents the standard deviation of the liquid velocity. Consequently, an iterative approach is typically required to determine ζ_l [15]. In particular, the process starts by calculating $\sigma_{\dot{U}}$ with an arbitrary value of ζ_l. Once $\sigma_{\dot{U}}$ is computed and substituted into Eq. (5), it yields a new value of ζ_l. This scheme is repeated iteratively until no significant differences in the calculation of ζ_l arise between successive iterations, resulting in a rather cumbersome procedure that complicates the optimal design of the STLCD device for vibration control purposes. In light of these considerations, a simplified optimization procedure for the STLCD device is proposed in the next section.

3 Optimal design of the STLCD control device

Determining the characteristic parameters of the STLCD control device under investigation is critical to achieving an optimal reduction in the response of the main system. As can be seen from Eq. (3), the response of the main system equipped with the STLCD is influenced by various parameters of the device, including the two mass ratios μ_l and δ, the natural frequency ω_l and the equivalent damping ratio of the liquid ζ_l, the length ratio α, the natural frequency ω_2 and the damping ratio ζ_2 of the STLCD container. However, due to structural and dimensional constraints, the values of μ_l, δ and α are tentatively set as constant [23,24]. As a result, only ζ_l, ζ_2, ω_l and ω_2 (or equivalently the frequency ratios $\nu_l = \omega_l / \omega_s$ and $\nu_2 = \omega_2 / \omega_s$, respectively) need to be appropriately optimized to effectively control the dynamic response. As usually done in the literature, these parameters can be determined by minimizing a specific objective function that measures the dynamic response of the structural system, such as the displacement or acceleration variance. In this regard, the total acceleration variance of the main SDOF structure is employed as the objective of the optimization procedure [25]. In order to find the optimal design parameters of the STLCD, Eq. (3) is written in compact matrix form as

$$\mathbf{M}\ddot{\mathbf{Z}}(t)+\mathbf{C}\dot{\mathbf{Z}}(t)+\mathbf{K}\mathbf{Z}(t)=-\mathbf{r}\ddot{X}_g(t) \tag{6}$$

where the matrices and vectors entering Eq. (6) are defined as

$$\mathbf{M}=\begin{bmatrix}1+\mu_t & \mu_t & \alpha\mu_l\\ 1 & 1 & \alpha\mu_l/\mu_t\\ \alpha & \alpha & 1\end{bmatrix};\mathbf{C}=\begin{bmatrix}2\zeta_s\omega_s & 0 & 0\\ 0 & 2\zeta_2\omega_2 & 0\\ 0 & 0 & 2\zeta_l\omega_l\end{bmatrix};\mathbf{K}=\begin{bmatrix}\omega_s^2 & 0 & 0\\ 0 & \omega_2^2 & 0\\ 0 & 0 & \omega_l^2\end{bmatrix};\mathbf{Z}(t)=\begin{bmatrix}X_s(t)\\ Y(t)\\ U(t)\end{bmatrix};\mathbf{r}=\begin{bmatrix}1+\mu_t\\ 1\\ \alpha\end{bmatrix} \tag{7}$$

By omitting time dependence for sake of conciseness and introducing the state vector $\mathbf{Q}=\begin{bmatrix}\mathbf{Z} & \dot{\mathbf{Z}}\end{bmatrix}^T$, the governing equations of motion can be written into the first-order state-space form as

$$\dot{\mathbf{Q}}=\mathbf{D}_\mathbf{S}\mathbf{Q}+\mathbf{G}_\mathbf{S}\ddot{X}_g \tag{8}$$

where $\mathbf{D}_\mathbf{S}$ and $\mathbf{G}_\mathbf{S}$ are given as [26]

$$\mathbf{D}_\mathbf{S}=\begin{bmatrix}\mathbf{0} & \mathbf{I}_3\\ \text{-}\mathbf{M}^{-1}\mathbf{K} & \text{-}\mathbf{M}^{-1}\mathbf{C}\end{bmatrix};\mathbf{G}_\mathbf{S}=\begin{bmatrix}\mathbf{0}\\ \mathbf{r}\end{bmatrix} \tag{9}$$

and $\mathbf{I}_3$ is a 3×3 identity matrix. The system response can be completely described by the covariance matrix $\mathbf{\Sigma}_\mathbf{Q}(t)=E\left[\mathbf{Q}\mathbf{Q}^T\right]$, where the symbol E[ ] denotes the expected value operator. Specifically, given that the input is modelled as a zero-mean stationary Gaussian white noise process, the corresponding Lyapunov equation describing the evolution of the covariance matrix can be written as [15,26]

$$\dot{\mathbf{\Sigma}}_\mathbf{Q}(t)=\mathbf{D}_\mathbf{S}\mathbf{\Sigma}_\mathbf{Q}(t)+\mathbf{\Sigma}_\mathbf{Q}(t)\mathbf{D}_\mathbf{s}^\mathbf{T}+\mathbf{G}_\mathbf{S}\mathbf{G}_\mathbf{S}^\mathbf{T}\pi G_0 \tag{10}$$

where the covariance matrix in terms of the state vector $\mathbf{\Sigma}_\mathbf{Q}(t)$ contains the variances of each response in terms of displacements and velocities on the principal diagonal and their covariances,

$$\boldsymbol{\Sigma}_{\mathbf{Q}}(t)=\begin{bmatrix} \sigma_{X_s}^2 & \sigma_{X_sY} & \sigma_{X_sU} & \sigma_{X_s\dot{X}_s} & \sigma_{X_s\dot{Y}} & \sigma_{X_s\dot{U}} \\ & \sigma_{Y}^2 & \sigma_{YU} & \sigma_{Y\dot{X}_s} & \sigma_{Y\dot{Y}} & \sigma_{Y\dot{U}} \\ & & \sigma_{U}^2 & \sigma_{U\dot{X}_s} & \sigma_{U\dot{Y}} & \sigma_{U\dot{U}} \\ & & & \sigma_{\dot{X}_s}^2 & \sigma_{\dot{X}_s\dot{Y}} & \sigma_{\dot{X}_s\dot{U}} \\ & sym & & & \sigma_{\dot{Y}}^2 & \sigma_{\dot{Y}\dot{U}} \\ & & & & & \sigma_{\dot{U}}^2 \end{bmatrix} \tag{11}$$

Considering that only the steady-state variance must be calculated, $\dot{\boldsymbol{\Sigma}}_{\mathbf{Q}}(t)$ can be set equal to zero and in this manner, the solution of Eq. (10) yields all the response statistics of the system in Eq. (6).

Focusing on the optimization procedure in detail, the STLCD device is designed in such a way that the total acceleration variance of the structural SDOF, namely, $\ddot{U}_{s,tot}=\ddot{X}_s+\ddot{X}_g$ is minimized [25]. Examining the first row in Eq. (1), the sought acceleration variance can be expressed as

$$\sigma_{\ddot{U}_{s,tot}}^2=E[\ddot{U}_{s,tot}{}^2]=E\left[\left(-2\zeta_s\omega_s\dot{X}_s-\omega_s{}^2X_s+\mu_t\omega_2{}^2Y+2\zeta_2\omega_2\mu_t\dot{Y}\right)^2\right] \tag{12}$$

By expanding the product in Eq. (12), the variance can be obtained as

$$\begin{aligned}\sigma_{\ddot{U}_{s,tot}}^2=&\ \omega_s^4\sigma_{X_s}^2-2\sigma_{X_sY}\mu_t\nu_2^2\omega_s^4+\mu_t^2\nu_2^4\sigma^2{}_Y\omega_s^4+4\sigma_{\dot{Y}}^2\zeta_2^2\mu_t^2\nu_2^2\omega_s^2-4\sigma_{X_s\dot{Y}}\zeta_2\mu_t\nu_2\omega_s^3+\\&+4\sigma_{Y\dot{Y}}\zeta_2\mu_t^2\nu_2^3\omega_s^3+4\sigma_{\dot{X}_s}^2\zeta_s^2\omega_s^2-8\sigma_{\dot{X}_s\dot{Y}}\zeta_2\zeta_s\mu_t\nu_2\omega_s^2+4\sigma_{X_s\dot{X}_s}\zeta_s\omega_s^3-4\sigma_{Y\dot{X}_s}\zeta_s\mu_t\nu_2^2\omega_s^3\end{aligned} \tag{13}$$

which involves the covariance of both the displacement responses and the velocity responses. In this form, the minimization of the variance is quite complex and must be calculated numerically using algorithms that might lead to cumbersome and time-consuming computations during the design phase [15,16].

Furthermore, as far as the optimization of the equivalent damping ratio ζ_l is concerned, an iterative approach should be pursued. Indeed, as previously mentioned, $\sigma_{\ddot{U}}$ remains unknown and implicitly depends on ζ_l, making the use of Eq. (5) for design purposes nontrivial [15,16]. Hence, to facilitate the estimation of the optimal STLCD parameters, a direct analytical approach is proposed. In particular, to directly determine the optimal parameters of the STLCD, it is essential to obtain an analytical expression of the total acceleration variance. For this purpose, some reasonable approximations can be introduced, as is common in many optimization procedures for passive vibration control systems [23,24]. Specifically, the SDOF main system is assumed to be undamped ($\zeta_s=0$), and considering that the damping effect of the liquid is typically small [27], the presence of the damping term is neglected at this stage ($\zeta_l=0$). It follows that the desired acceleration variance in Eq (13) can be simplified as

$$\tilde{\sigma}_{\ddot{U}_{s,tot}}^2=\omega_s^4\sigma_{X_s}^2+\mu_t\nu_2\omega_s^2\left(-2\nu_2\omega_s^2\sigma_{X_sY}+\mu_t\nu_2^3\omega_s^2\sigma^2{}_Y+4\zeta_2\left(\zeta_2\mu_t\nu_2\sigma_{\dot{Y}}^2-\omega_s\sigma_{X_s\dot{Y}}\right)\right) \tag{14}$$

where the covariances in Eq. (14) can be found in closed form as solution of the Lyapunov equation presented in Eq.(10). Hence, after some algebra, the total acceleration variance can be derived in an analytical form as

$$\tilde{\sigma}_{\ddot{U}_{s,tot}}^2=\frac{\pi G_0\omega_s}{4z_{\ddot{U}_{s,tot}}} \tag{15}$$

in which

$$z_{\ddot{U}_{s,tot}}=\frac{N_{z_{\ddot{U}_{s,tot}}}}{D_{z_{\ddot{U}_{s,tot}}}} \tag{16}$$

is independent to both the intensity G_0 and the natural frequency of the main system ω_s, as it can be seen from the numerator and denominator,

$$N_{z_{\ddot{U}_{s,tot}}} = \zeta_2 \mu_t \nu_2 \left(\alpha^2 \mu_l + \mu_t \left(-1 + \nu_l^2 \right) \right)^2$$

$$D_{z_{\ddot{U}_{s,tot}}} = \alpha^4 \mu_l^2 \left(1 + \mu_t \nu_2^2 \left(-1 + \mu_t \nu_2^2 \right) \right) + \mu_t^2 \left(1 + \left(-2 - \mu_t + 4\zeta_2^2 \left(1 + \mu_t \right) \right) \nu_2^2 + \left(1 + \mu_t \right)^2 \nu_2^4 \right) \left(-1 + \nu_l^2 \right)^2 +$$
$$+ \alpha^2 \mu_l \mu_t \left(-2 + 2\left(1 + \mu_t - 2\zeta_2^2 \mu_t \right) \nu_2^2 - 2\mu_t \left(1 + \mu_t \right) \nu_2^4 + \left(2 + \nu_2^2 \left(-2 + \mu_t \left(-2 + 8\zeta_2^2 + \left(3 + 2\mu_t \right) \nu_2^2 \right) \right) \right) \nu_l^2 \right)$$

To find the minimum of the total acceleration variance, the maximum of the function $z_{\ddot{U}_{s,tot}}\left(\zeta_2, \nu_l, \nu_2\right)$ can be sought by considering its relationship in Eq. (15). In this regard, a sample of the function $z_{\ddot{U}_{s,tot}}\left(\zeta_2, \nu_l, \nu_2\right)$ is presented in Fig. 3. Specifically, the search for the optimal design parameter ζ_2, ν_l, ν_2 and the maximization $z_{\ddot{U}_{s,tot}}\left(\zeta_2, \nu_l, \nu_2\right)$ involves solving the following equations,

$$\begin{cases} \partial z_{\ddot{U}_{s,tot}}\left(\zeta_2, \nu_l, \nu_2\right) / \partial \zeta_2 = 0 \\ \partial z_{\ddot{U}_{s,tot}}\left(\zeta_2, \nu_l, \nu_2\right) / \partial \nu_2 = 0 \\ \partial z_{\ddot{U}_{s,tot}}\left(\zeta_2, \nu_l, \nu_2\right) / \partial \nu_l = 0 \end{cases} \quad \text{(17a-c)}$$

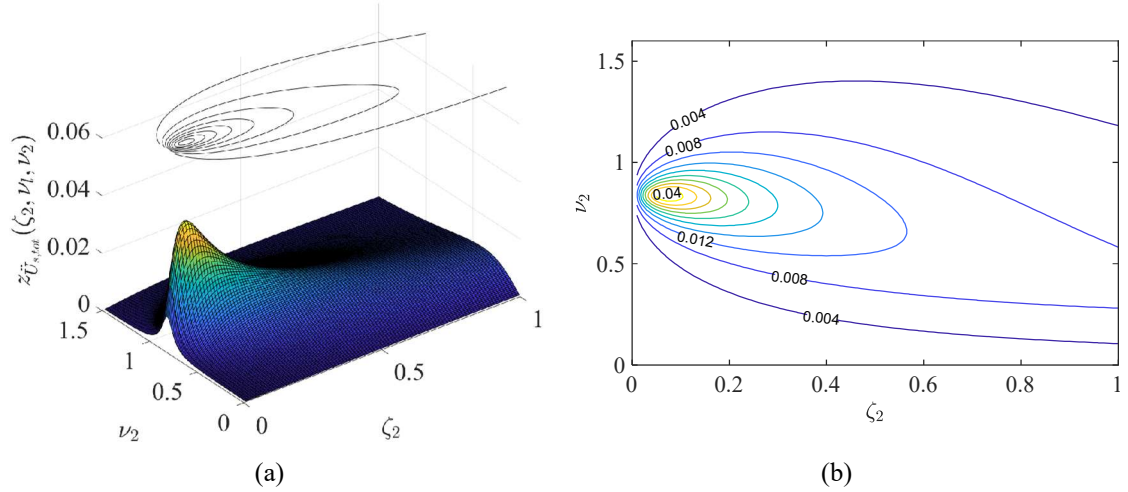

(a) (b)

Fig.3 (a) Sample of the function $z_{\ddot{U}_{s,tot}}\left(\zeta_2, \nu_l, \nu_2\right)$; (b) contour plot of $z_{\ddot{U}_{s,tot}}\left(\zeta_2, \nu_l, \nu_2\right)$ on the ζ_2 - ν_2 plane (for α =0.6, δ =0.01, L =12 m, ω_s =20.94 rad/s, μ_l =0.03, ν_l =0.061)

In detail, from Eqs. (17)a-(17)b an analytical expression of the optimal parameters $\tilde{\nu}_{2,opt}\left(\nu_l\right)$ and $\tilde{\zeta}_{2,opt}\left(\nu_l\right)$ as functions of ν_l can be found as

$$\tilde{\nu}_{2,opt}\left(\nu_l\right) = \sqrt{A / B} \quad \text{(18a-c)}$$

with

$$A=\left(\alpha^2\mu_l+\mu_t\left(-1+\nu_l^2\right)\right)\left(\alpha^2\mu_l+\left(2+\mu_t\right)\left(-1+\nu_l^2\right)\right);$$

$$B=2\mu_t\left(\alpha^4\mu_l^2+\left(1+\mu_t\right)^2\left(-1+\nu_l^2\right)^2+\alpha^2\mu_l\left(-2\left(1+\mu_t\right)+\left(3+2\mu_t\right)\nu_l^2\right)\right);$$

and

$$\tilde{\zeta}_{2,opt}\left(\nu_l\right)=\sqrt{C/D} \tag{19a-c}$$

with

$$C=-3\alpha^6\mu_l^3-\mu_t^2\left(4+3\mu_t\right)\left(-1+\nu_l^2\right)^3-\alpha^2\mu_l\mu_t\left(-1+\nu_l^2\right)\left(-8-9\mu_t+3\left(4+3\mu_t\right)\nu_l^2\right)+$$
$$+\alpha^4\mu_l^2\left(4+9\mu_t-\left(8+9\mu_t\right)\nu_l^2\right);$$

$$D=-8\mu_t\left(\left(1+\mu_t\right)\left(2+\mu_t\right)\left(-1+\nu_l^2\right)^3+\alpha^4\mu_l^2\left(-1+2\nu_l^2\right)+\alpha^2\mu_l\left(-1+\nu_l^2\right)\left(-3-2\mu_t+\left(5+3\mu_t\right)\nu_l^2\right)\right)$$

In Figs. 4(a)-(b), the approximate solutions of the optimal parameters $\tilde{\nu}_{2,opt}\left(\nu_l\right)$ and $\tilde{\zeta}_{2,opt}\left(\nu_l\right)$ obtained by Eqs. (18)- (19), are shown for different values of μ_l.

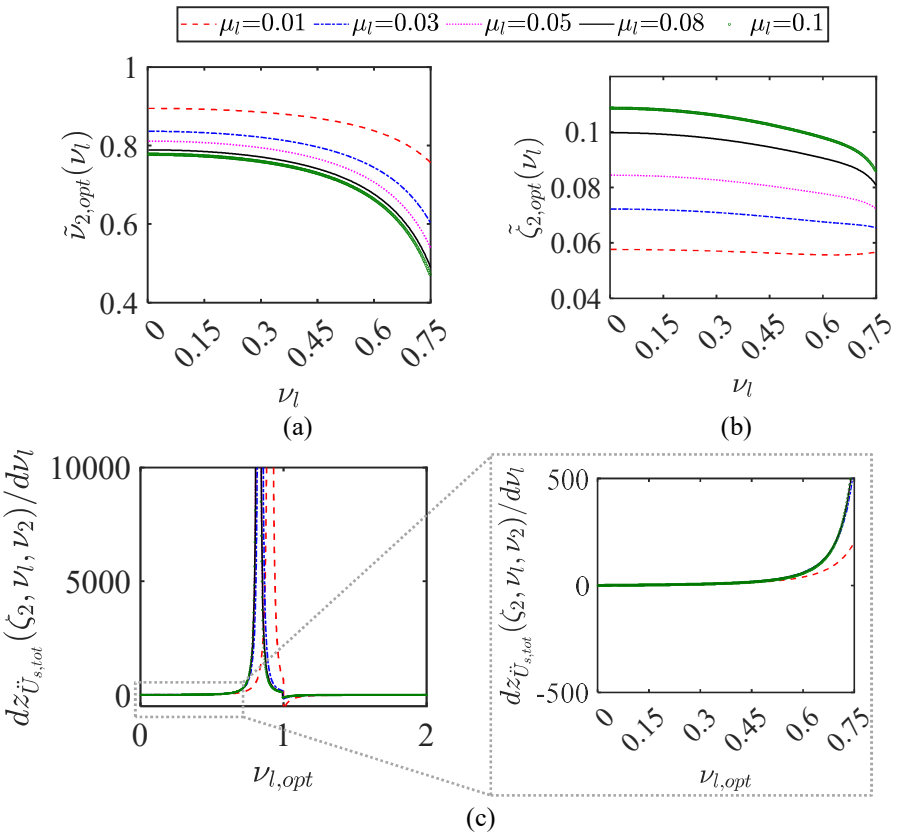

Fig.4 Approximated solutions of the STLCD optimal parameters for different values of μ_l (for α =0.6, δ =0.01, L =12 m, ω_s =20.94 rad/s, μ_l =0.03, ν_l =0.061): a) $\tilde{\nu}_{2,opt}\left(\nu_l\right)$; b) $\tilde{\zeta}_{2,opt}\left(\nu_l\right)$; c) trend of $\partial z_{\ddot{U}_{s,tot}}\left(\zeta_2,\nu_l,\nu_2\right)/\partial\nu_l$

As illustrated in Figs. 4(a)-(b), $\tilde{\nu}_{2,opt}(\nu_l)$ and $\tilde{\zeta}_{2,opt}(\nu_l)$ show opposite behavior with increasing values of μ_l, while both parameters maintain a nearly steady trend for each value of ν_l, suggesting that $\tilde{\nu}_{2,opt}(\nu_l)$ and $\tilde{\zeta}_{2,opt}(\nu_l)$ are largely unaffected by variation of ν_l within the practical range of interest. Finally, optimal values of $\nu_{l,opt}$ that maximize the function $z_{\ddot{U}_{s,tot}}(\zeta_2,\nu_l,\nu_2)$ can be similarly found by solving Eq. (17)c. However, due to the resulting complex expression, the analytical form of $\nu_{l,opt}$ is omitted here for brevity and only the trend of $\partial z_{\ddot{U}_{s,tot}}(\zeta_2,\nu_l,\nu_2)/\partial\nu_l$ is shown in Fig. 4(c). As evident, except for values near unity, where the derivative exhibits a discontinuity and solutions in terms of $\tilde{\nu}_{2,opt}(\nu_l)$ and $\tilde{\zeta}_{2,opt}(\nu_l)$ would assume imaginary values, a wide range of ν_l values ($\nu_l=\sqrt{2g/\left(L\omega_s^2\right)}$ <0.6, a realistically achievable value for short-period structures with practical liquid lengths) leads to values of $\partial z_{\ddot{U}_{s,tot}}(\zeta_2,\nu_l,\nu_2)/\partial\nu_l$ close to zero, implying that slight variations of ν_l in this range have minimal effect on reaching the maximum. Thus, once the value of $\nu_{l,opt}$ is determined based on the specific frequency of the main structure ω_s and the total length L suitable for the available space, Eqs. (18)-(19) can be used for a straightforward determination of the optimal STLCD design parameters $\tilde{\nu}_{2,opt}(\nu_l)$ and $\tilde{\zeta}_{2,opt}(\nu_l)$.

Regarding the determination of the optimal head loss coefficient, as previously elucidated, conventional methods calculate the equivalent damping ratio ζ_l by employing a time-consuming iterative process. Conversely, this study proposes a quicker alternative for the approximate estimation of ζ_l. Specifically, the optimal value of ζ_l is evaluated based on the analysis developed in [24] considering the SDOF structure with a classical TLCD subjected to white noise excitation. In this case, the total acceleration variance $\hat{\sigma}^2_{\ddot{U}_{s,tot}}$ of an SDOF system controlled by a TLCD device can be expressed as [15]

$$\hat{\sigma}^2_{\ddot{U}_{s,tot}}=\frac{\pi G_0\omega_s}{4\hat{z}_{\ddot{U}_{s,tot}}}; \tag{20}$$

where

$$\hat{z}_{\ddot{U}_{s,tot}}=\hat{N}_{\hat{z}_{\ddot{U}_{s,tot}}}/\hat{D}_{\hat{z}_{\ddot{U}_{s,tot}}} \tag{21}$$

with the numerators and denominators given by

$$\begin{aligned}\hat{N}_{\hat{z}_{\ddot{U}_{s,tot}}}=&\left(-1+\left(-1+\alpha^2\right)\mu_l\right)(\zeta_l\zeta_s+\zeta_l^2\left(4\zeta_s^2+\alpha^2\mu_l\right)\nu_l+2\zeta_l\zeta_s\left(-1+2\zeta_s^2+\left(-1+\alpha^2\right)\mu_l+2\zeta_l^2\left(1+\mu_l\right)\right)\nu_l^2+\\&+\zeta_s^2\left(\alpha^2\mu_l+4\zeta_l^2\left(1+\mu_l\right)\right)\nu_l^3+\zeta_l\zeta_s\left(1+\mu_l\right)^2\nu_l^4);\end{aligned}$$

$$\begin{aligned}\hat{D}_{\hat{z}_{\ddot{U}_{s,tot}}}=&4\zeta_l^3\left(1+4\zeta_s^2+\mu_l\right)\left(-1+\left(-1+\alpha^2\right)\mu_l\right)\nu_l^2+\alpha^2\zeta_s\mu_l\left(-1-4\zeta_s^2+\left(-1+\alpha^2\right)\mu_l\right)\nu_l^3+\\&+4\zeta_l^2\zeta_s\nu_l\left(-1-4\zeta_s^2-\mu_l+\alpha^2\mu_l+\left(1+4\zeta_s^2+\mu_l\right)\left(-1+\left(-1+\alpha^2\right)\mu_l\right)\nu_l^2\right)+\\&+\zeta_l\left(-16\zeta_s^4\nu_l^2+\left(-1+\left(-1+\alpha^2\right)\mu_l\right)\left(1+\left(-2+\left(-2+\alpha^2\right)\mu_l\right)\nu_l^2+\left(1+\mu_l\right)^2\nu_l^4\right)+\\&+4\zeta_s^2\left(-1+\left(-1+\left(-1+\alpha^2\right)\mu_l\right)\nu_l^2\left(-1+\left(1+\mu_l\right)\nu_l^2\right)\right));\end{aligned}$$

At this point, the optimal value of the equivalent damping ratio ζ_l can be obtained without resorting to iteration by searching for the maximum of $\hat{z}_{\dot{U}_{s,tot}}$ in Eq. (21) as

$$\zeta_{l,opt} = \frac{\sqrt{1-2\nu_l^2-2\mu_l\nu_l^2+\alpha^2\mu_l\nu_l^2+\nu_l^4+2\mu_l\nu_l^4+\mu_l^2\nu_l^4}}{2\sqrt{\nu_l^2+\mu_l\nu_l^2}} \tag{22}$$

Next, by setting this value in Eq. (5), the value of $\tilde{\xi}_{opt}$ can be evaluated as

$$\tilde{\xi}_{opt} = 2L\zeta_{l,opt}\nu_{l,opt}\omega_s\sqrt{\pi/\left(2\hat{\sigma}_{\dot{U}}\right)} \tag{23}$$

where $\hat{\sigma}_{\dot{U}}^2$ is the variance of the fluid velocity of the system with TLCD, which can be obtained in the form [15]

$$\hat{\sigma}_{\dot{U}}^2 = \frac{\pi G_0}{4\nu_l\omega_s\hat{z}_{\dot{U}}}; \tag{24}$$

with

$$\hat{z}_{\dot{U}} = \hat{N}_{\hat{z}_{\dot{U}}} / \hat{D}_{\hat{z}_{\dot{U}}} \tag{25}$$

and

$$\hat{N}_{\hat{z}_{\dot{U}}} = 4\zeta_l^3\zeta_s\left(1+\mu_l\right)\nu_l^2+\alpha^2\zeta_s^2\mu_l\nu_l^3+\zeta_l\zeta_s\left(1+2\left(-1+2\zeta_s^2+\left(-1+\alpha^2\right)\mu_l\right)\nu_l^2+\left(1+\mu_l\right)^2\nu_l^4\right)+$$
$$+\zeta_l^2\nu_l\left(\alpha^2\mu_l+4\zeta_s^2\left(1+\left(1+\mu_l\right)\nu_l^2\right)\right);$$
$$\hat{D}_{\hat{z}_{\dot{U}}} = \alpha^2\left(\zeta_s+4\zeta_l\zeta_s^2\nu_l+\zeta_l\left(1+\mu_l\right)\nu_l+4\zeta_s^3\nu_l^2\right);$$

As will be demonstrated in the next section, this approach leads to almost identical outcomes in terms of total acceleration variance compared to conventional iterative techniques without compromising the effectiveness of the STLCD.

4 Numerical validation

In this section, the proposed optimization procedure is validated through numerical simulations. To demonstrate its accuracy, the results in terms of total acceleration variance obtained by employing the proposed optimal STLCD design parameters $\tilde{\nu}_{2,opt}\left(\nu_l\right)$, $\tilde{\zeta}_{2,opt}\left(\nu_l\right)$, and $\tilde{\xi}_{opt}$, are compared with the optimal values obtained through a numerical iterative approach. The optimal STLCD parameters were estimated taking into account the characteristics of the SDOF structure and the STLCD device examined in [21] as a reference. Specifically, the natural period of the structure T_s is 0.3 s (ω_s =20.94 *rad/s*) and a structural damping ζ_s of 1% was considered. Based on the analytical solutions provided in Eqs. (18)-(19)-(23), the optimal STLCD design parameters have been calculated assuming that the liquid is water ($\rho = 997$ kg/m^3) and the total length is $L = 10$ m. A feasible value of the liquid mass ratio $\mu_l = 0.05$ has been assumed and the STLCD container mass is considered equal to the liquid mass, thus, $\delta = 0.05$. Moreover, the ratio of the horizontal length to the total length of the liquid column tube, α, is assumed to be a commonly used value of 0.9. Additionally, to calculate the total acceleration variance the Power Spectral Density (PSD) intensity is set equal to $G_0 = 0.002$ m^2/s^3.

With reference to the previously considered structural parameters, the optimal STLCD design parameters determined through the proposed method have been used to compute the total acceleration variance $\sigma_{\dot{U}_{s,tot}}^2$ in Eq. (13). It is worth noting that the optimal STLCD parameters in Eqs. (18)-(19) do not depend on ω_s, ζ_s, G_0, and ζ_l, and are therefore assumed to be constant as these parameters vary. Since these terms were previously neglected to derive the proposed approximate expressions of the STLCD parameters, the reliability of the proposed formulation may be compromised especially when they assume relatively high values. Furthermore, as discussed earlier, the optimal frequency ratio of the liquid $\nu_{l,opt}$ can be varied over a wide range of values, which

can differ significantly depending on the feasible lengths of the liquid tank L. Therefore, a parametric analysis has been conducted to evaluate mainly the impact of ν_l, ω_s, ζ_s, G_0, ζ_l, and the other parameters α, δ and μ_l on the variance estimation. Each one of them was varied within a plausible range of values greater than zero, since they cannot take negative values. On the other hand, the numerical solution in terms of optimal STLCD parameters that minimize the total acceleration variance in Eq. (13), can be obtained by a control algorithm. In this respect, the particle-swarm optimization (PSO) method was employed [28,29].

Obviously, the implementation of this numerical minimization algorithm requires the imposition of certain constraints on the optimal parameters sought for the STLCD. The numerical optimal values of $\tilde{\nu}_{2,opt}$, and $\tilde{\zeta}_{2,opt}$ are sought in the range 0.01-1, while the limits for the head loss coefficient are chosen according to the empirical data of [12] and the equivalent damping ratio is limited by the maximum value of $\zeta_l = 1$ [16]. It should be emphasized that each iteration of the numerical algorithm yields an optimal value of ξ_{opt}, which requires an iterative application of the SLT to evaluate the equivalent linear damping ratio ζ_l, and results in a cumbersome numerical procedure. Next, the control performance of the STLCD-controlled structure is assessed by examining the values assumed by a performance index $\eta_{\sigma_{\ddot{U}_{s,tot}}}$ that quantifies the vibration reduction achieved by the structure controlled with STLCD compared to the same structure without the control device. This performance index is calculated as $\eta_{\sigma_{\ddot{U}_{s,tot}}} = \sigma^2_{\ddot{U}_{s,tot}} \Big/ \sigma^2_{\ddot{U}_{s0,tot}}$ where $\sigma^2_{\ddot{U}_{s0,tot}} = E[\ddot{U}_{s0,tot}] = 4\zeta_s{}^2\omega_s{}^2\sigma^2_{\dot{x}_{s0}} + \omega_s{}^4\sigma^2_{x_{s0}}$ [25] represents the acceleration variance of the system without STLCD and $\sigma^2_{\dot{x}_{s0}}$ and $\sigma^2_{x_{s0}}$ are the variances in terms of relative velocity and displacement, respectively. Note that lower values of $\eta_{\sigma_{\ddot{U}_{s,tot}}}$ indicate higher control effectiveness of the STLCD.

The comparisons between the normalized acceleration variance obtained by the numerical procedure (black solid line with square markers) and that one calculated using the proposed analytical solutions of the optimal STLCD parameters (red dots with circular markers) are illustrated in Fig. 5 for various values of ω_s, ζ_s, G_0, ζ_l, ν_l, α, δ and μ_l. In all the graphs, it can be seen that the control performance index values $\eta_{\sigma_{\ddot{U}_{s,tot}}}$ are always lower than 1, confirming the efficacy of the STLCD device in mitigating the accelerations compared to the uncontrolled system. It is worth highlighting that the absolute percentage calculated error as $\left|\eta^{num}{}_{\sigma_{\ddot{U}_{s,tot}}} - \eta^{prop}{}_{\sigma_{\ddot{U}_{s,tot}}}\right| \cdot 100$, where $\eta^{num}{}_{\sigma_{\ddot{U}_{s,tot}}}$ is the maximum acceleration variance derived from the numerical procedure and $\eta^{prop}{}_{\sigma_{\ddot{U}_{s,tot}}}$ that obtained by the proposed analytical solutions for the optimal STLCD parameters, remains below 2% over various values of ζ_l and below 10 % for ν_l (Fig. 5 (a)-(b)). This suggests that the recommendation to determine the optimal values of ν_l based on practical constraints related to the length of the column liquid and the period of the structure, and to extract the equivalent damping ratio ζ_l from the corresponding system controlled by a traditional TLCD, does not compromise the reliability of the predicted response. Moreover, consistent results are observed for other parameters (discrepancies below 2% for different values of α, G_0, μ_l, 4% for δ and ω_s, and 8% for ζ_s), with the most significant discrepancy occurring at very high values of the frequency ratio ν_l. However, since these discrepancies are consistently kept below 10%, the suggested optimization method can be considered as practically equivalent to the numerical approach in terms of control performance. It is worth mentioning that the optimal STLCD parameters found by the numerical approach are obtained by considering the original damped structure with the nonlinear dynamic behavior governed by Eq. (2). Hence, the damping of the structure leads to increased computational times to minimize the variance. Moreover, this numerical algorithm must be adapted to the new structural configuration for each potential variation of each parameter and repeated accordingly. Conversely, the proposed approach provides a direct formula that can be readily utilized for the STLCD design. Therefore, considering the substantial computational gain achieved by the proposed approximate formulation, it can be concluded that the analytical expressions provided in Eqs. (18)-(19)-(23) can be used as a practical convenient tool for the optimal design of the STLCD.

The above proposed optimization procedure has been derived considering a white noise base excitation, which leads to the simplified analytical expressions in Eqs. (18)-(19)-(23) with minimal computational expense. In light of this, in order to study the robustness of the optimized STLCD for vibration control of short-period

structures and the validity of the proposed formulation, an experimental investigation was conducted on small-scale models, as shown in the following.

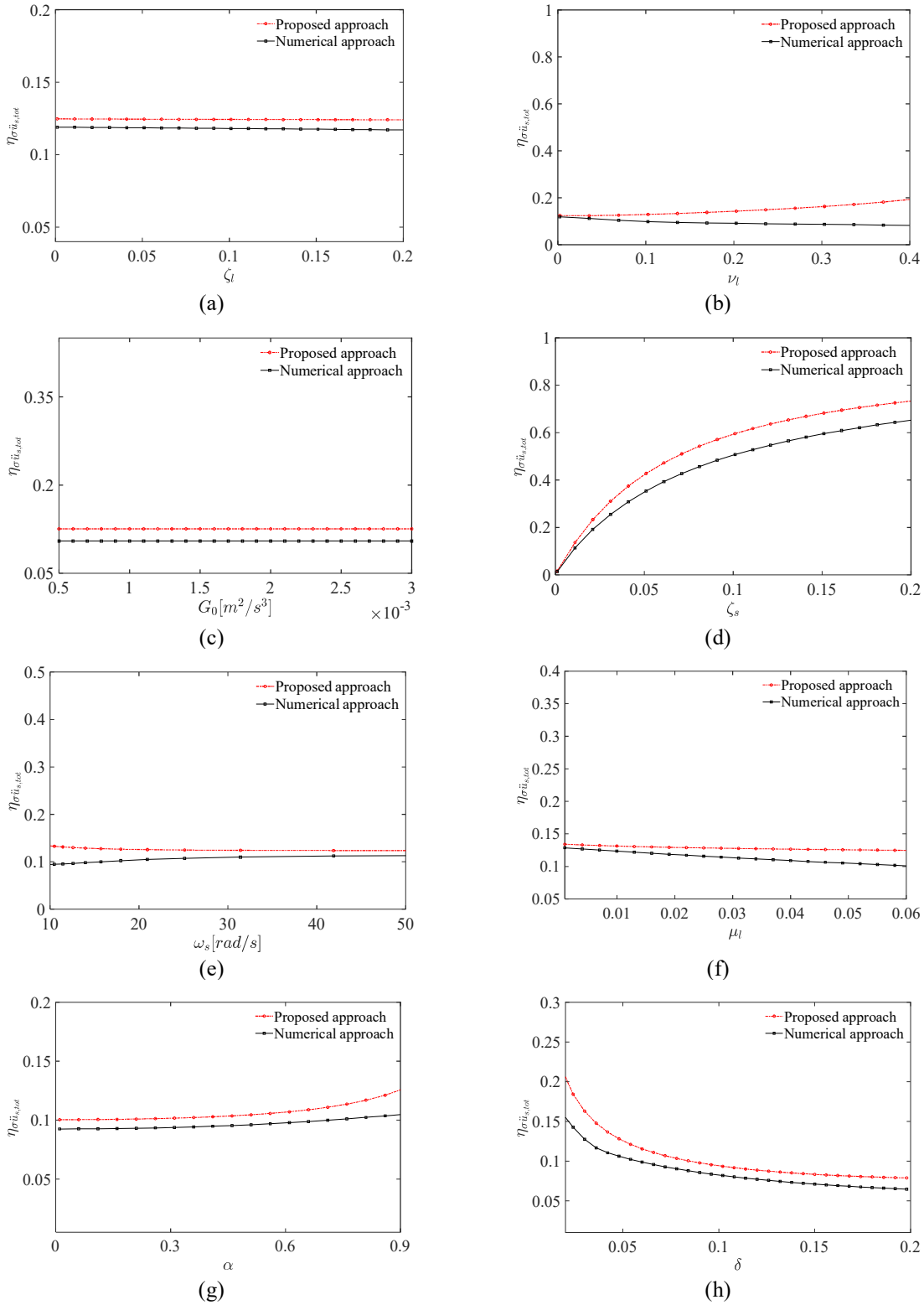

Fig.5 Normalized acceleration variance of the main system. Comparison between the numerical procedure (black solid line with squared markers) and the proposed formulation (red dash-dotted line with dots) varying

the system parameters. Reference set of parameters: G_0 =0.002 m^2/s^3; L = 10 m; δ =0.05; μ_l =0.05; ω_s =20.94 rad/s; ζ_s =0.01; α =0.9.

5 Experimental investigation

5.1 Description of the scale model and the experimental set-up

This section presents the experimental tests conducted on a small-scale model of an STLCD-controlled structure to investigate the effectiveness of the proposed optimized STLCD device for vibration control of stiff structures. First, two subsystems, namely, the benchmark SDOF structure (Fig. 6) and the STLCD device (Fig. 7), were investigated and tested individually. The benchmark SDOF structure, illustrated in Fig. 6, is composed of a single-story, single-bay frame structure. Two plexiglass plates, each 300 mm wide and 15×300 mm in section, represent the base and the roof. Two pairs of aluminium elements with a height of 300 mm and a rectangular section of 70×0.5 mm serve as vertical supports connecting the top plate to the base. For comparison purposes, a 200 mm long linear guide is attached to the top plate, which serves as a support for the STLCD control device to be studied. In this manner, the mass of the linear guide is included in the total mass of the structure.

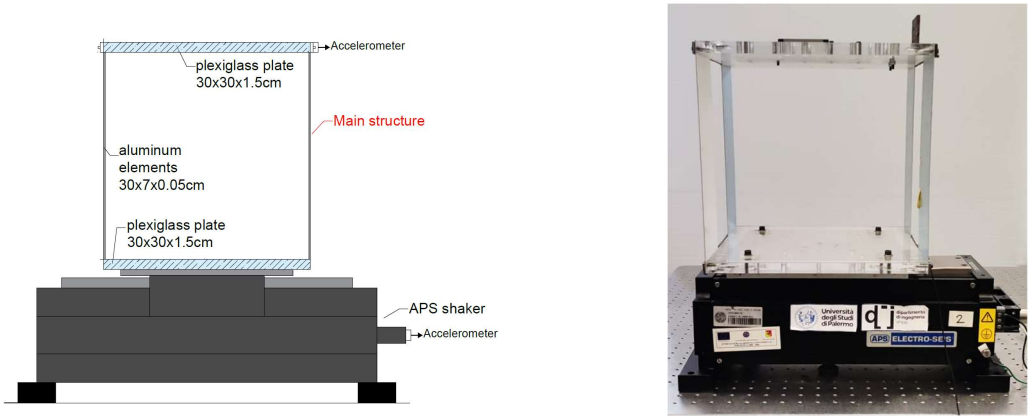

Fig. 6 Small-scale model of the benchmark SDOF structure

From a practical point of view, the STLCD device (Fig. 7) was realized using a U-shaped acrylic glass container with a constant rectangular cross-section. The container was filled with water, and a few drops of lubricant fluid were added to the water to enhance the contrast and provide a reflecting surface that allows an optical laser to analyze the reflected signal. The device support is free to move, and it is connected to the support plate through a spring (length 50 mm, diameter 10 mm, stiffness 0.2 N/mm). The spring and the total mass of the device were chosen according to the optimal tuning described in the previous sections. The dashpots depicted in the mathematical models in Fig. 2 were not realized. Thus, the inherent damping was estimated based on the intrinsic properties of the systems. By successively assembling the two subsystems, the benchmark SDOF structure (Fig. 6) and the STLCD device (Fig. 7), the whole STLCD-controlled structure as illustrated in Fig. 8 was realized and analyzed in its entirety.

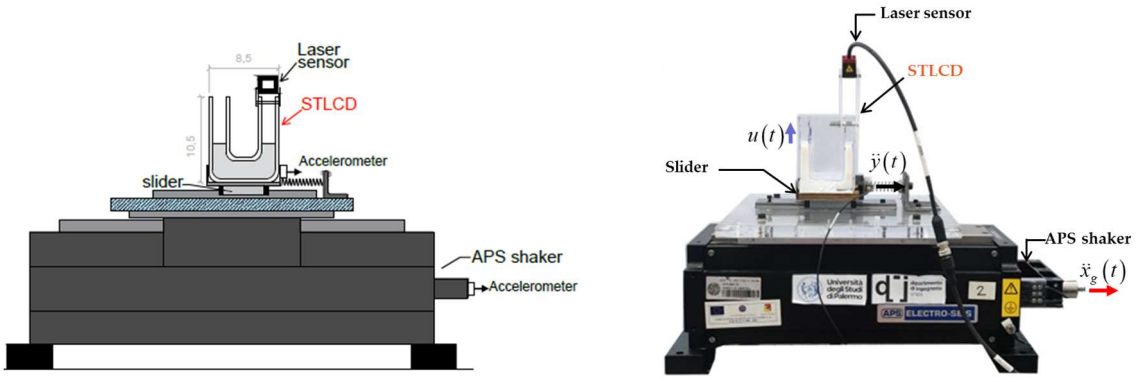

Fig. 7 Small-scall model of the proposed STLCD device

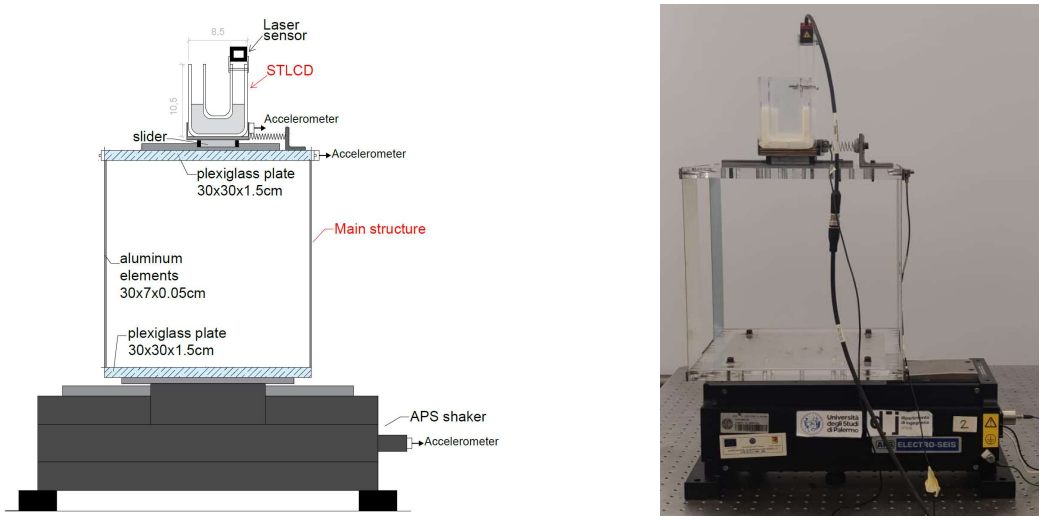

Fig. 8 Small-scale model of the STLCD-controlled structure

In order to assess the validity of the proposed mathematical models, identification procedures are applied to numerically evaluate the parameters of each one of the subsystems and of the complete STLCD-controlled structure, so that the theoretical dynamic response of the scale model matches the experimental measurement data. The parameters to be identified are mainly the fundamental frequencies and damping ratios, and they are found separately for each subsystem, given the other known structural and geometrical properties, which are summarized in Table 1.

Table 1. Reference parameters for the primary SDOF structure and STLCD device

SDOF structure	Total mass	$M_s = 3.449\,\text{kg}$
STLCD	Liquid mass ratio	$\mu_l = \rho AL / M_s = 0.034$
	Container mass ratio	$\delta = M_c / M_s = 0.095$
	Total mass ratio	$\mu_t = \mu_l + \delta = 0.13$
	Length ratio	$\alpha = L_h / L = 0.48$

The experimental tests were carried out at the Laboratory of Experimental Dynamics, University of Palermo using the APS 113 ELECTRO-SEIS shaker providing the base excitation. During testing, the total lateral

accelerations of the shake table, the roof, and the sliding STLC container were recorded by two types of piezo-electric accelerometers, i.e., DeltaTron Accelerometers Brüel&Kjaer Type 4507-002B and PCB-Type 393B04, respectively. The first type was used to acquire the accelerations of the device and roof of the structure, while the second type was used to measure the acceleration of the shake table. Moreover, an optical laser sensor of type optoNCDT 1420-500, manufactured by Micro-Epsilon Messtechnik GmbH, was attached to one column of the STLCD to measure the vertical liquid displacement. The signal data originating from the accelerometers was acquired by an NI PXIe-1082 DAQ device, equipped with a high-performance multi-channel NI PXIe-4497 board. Finally, the entire system was controlled by ad-hoc developed signal processing software in the LabVIEW environment.

5. 2 Dynamic identification of the benchmark SDOF structure and the STLCD device

This section first describes the dynamic identification technique used to determine the fundamental parameters of the benchmark structure through shake table tests and validates the mathematical model. Subsequently, the dynamic identification of the parameters of the STLCD device is performed and the mathematical models are verified analogously through shake table tests.

The first phase of experimentation involved the dynamic identification of the SDOF scale model (Fig. 5 (a)). The linear dynamic response of the system is described by using the following mathematical model [30],

$$\ddot{x}_s(t) + 2\zeta_s\omega_s\dot{x}_s(t) + \omega_s{}^2 x_s(t) = -\ddot{x}_g(t) \tag{26}$$

The natural frequency and the damping ratio of the structure, ω_s and ζ_s, are the parameters to be identified. For their identification, the experimental model was subjected to a broadband noise as ground acceleration $\ddot{x}_g(t)$, ranging from 0.1 to 15 Hz in 20 seconds, supplied by the APS Shake Table II. Ten tests were performed and the ground acceleration (i.e., the shake table acceleration) and roof acceleration were recorded. The experimental frequency response functions (FRF) of the roof accelerations were calculated using the *tfestimate (Transfer function estimate)* built-in command in MatLab [31], taking the ground acceleration as the input signal. The objective that the mean experimental FRF and analytical FRF $H_{\ddot{X}_{s0}}(\omega)$ given by

$$H_{\ddot{X}_{s0}}(\omega) = \frac{-\omega^2}{\omega_s^2 - \omega^2 + 2i\omega\zeta_s\omega_s} \tag{27}$$

match provides the parameters to be identified. This match was performed using the nonlinear least square curve fitting method [32] (implemented with the *lsqcurvefit* built-in command in MatLab), resulting in the following frequency ω_s=19.13 rad/s (T_s=0.33 s) and damping ratio ζ_s=0.012. As can be seen from Fig. 9(a), the FRF computed with Eq. (26) (i.e., analytical solution, shown by dash-dotted lines) based on these parameters is in excellent agreement with the experimental one (dotted lines). For the sake of completeness, Fig. 9(b) also shows a comparison of the time history response in terms of roof absolute acceleration, obtained numerically by solving Eq. (25) with the *ode45* built-in command in MatLab [33]. Full agreement between the numerical and recorded acceleration is also observed in the time domain.

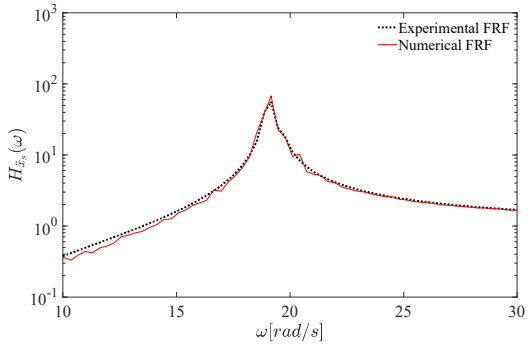

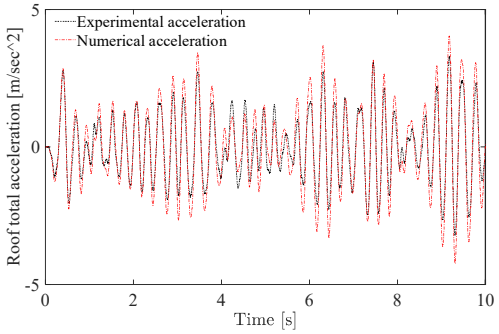

(a) (b)

Fig. 9 Total acceleration response of the SDOF system in terms of (a) FRF; (b) time history

In order to reduce the accelerations of this structure, an STLCD control device was properly designed. In fact, it should be noted that the use of a TLCD would not be possible in this case because the total length of the liquid inside the container should be $L \simeq 5$ cm for optimal tuning ($\omega_l \simeq \sqrt{2g/L} \simeq \omega_s$), which is difficult to achieve in practice. On the other hand, considering the liquid mass ratio as $\mu_l = 0.034$, the total mass ratio $\mu_t = 0.13$ and the length ratio set as $\alpha = 0.48$, the spring constant of the STLCD was set in such a way that $\omega_2 \simeq 0.8\omega_s$ according to the optimal tuning procedure proposed in this paper. As mentioned above, in order to fully characterize the STLCD device, the damping ratio ζ_l , the frequency ω_l of the liquid in the container, the damping ratio ζ_2 and the frequency ω_2 of the STLCD container can be determined by studying the dynamic behavior of the stand-alone STLCD using the following equivalent linear model

$$\begin{cases} \ddot{y}(t) + \alpha\mu_l \ddot{u}(t)/\mu_t + 2\zeta_2\omega_2\dot{y}(t) + \omega_2^2 y(t) = -\ddot{x}_g(t) \\ \alpha\ddot{y}(t) + \ddot{u}(t) + 2\zeta_l\omega_l\dot{u}(t) + \omega_l^2 u(t) = -\alpha\ddot{x}_g(t) \end{cases} \tag{28}$$

In the underlying tests, the STLCD is investigated through base excitation by the APS shaker as depicted in Fig. 6. In order to apply the SLT, the STLCD is subjected to a band-limited white noise base excitation with a frequency range of 0.1-15 Hz. Specifically, ten samples of broadband noise with a duration of 20 s were generated and used as ground acceleration. Low-amplitude dynamic tests were conducted to prevent water from spilling out of the STLCD container. In this way, sloshing effects can be considered negligible since they are usually associated with large amplitude excitations. For each sample, the ground acceleration, the container acceleration, and the free water surface displacement were recorded by the accelerometers and the optical sensor, respectively. Based on these data, the averaged experimental FRF was computed using the ground acceleration as the input signal and the liquid column displacement or the STLCD acceleration as the output signal. The STLCD parameters are determined with the nonlinear least square curve fitting method by imposing a match between the experimentally FRFs of the acceleration of the STLCD container and the liquid displacement and their analytical counterparts,

$$H_{\ddot{y}}(\omega) = \frac{-\alpha^2\omega^4\mu_l - \omega^2\mu_t\left(-\omega^2 + 2\mathrm{i}\omega\zeta_l\omega_l + \omega_l^2\right)}{\alpha^2\omega^4\mu_l - \mu_t\left(-\omega^2 + 2\mathrm{i}\omega\zeta_2\omega_2 + \omega_2^2\right)\left(-\omega^2 + 2\mathrm{i}\omega\zeta_l\omega_l + \omega_l^2\right)} \tag{29a-b}$$

$$H_U(\omega) = \frac{\alpha\mu_t\left(2\mathrm{i}\omega\zeta_2\omega_2 + \omega_2^2\right)}{\alpha^2\omega^4\mu_l - \mu_t\left(-\omega^2 + 2\mathrm{i}\omega\zeta_2\omega_2 + \omega_2^2\right)\left(-\omega^2 + 2\mathrm{i}\omega\zeta_l\omega_l + \omega_l^2\right)} \tag{29a-b}$$

The identified damping ratio and frequency of the liquid and of the STLCD container are ζ_l =0.023, ω_l =11.74 rad/s, ζ_2 =0.079 and ω_2 =15.49 rad/s, respectively. Figs. 10 (a)-(b) and Figs. 10 (c)-(d) show the liquid response and the acceleration of the STLCD container in frequency and time domain. As can be seen, the experimental and numerical responses agree satisfactorily in both domains, confirming that the approximate linear behavior of the fluid column is sufficiently accurate to model the STLCD response as well.

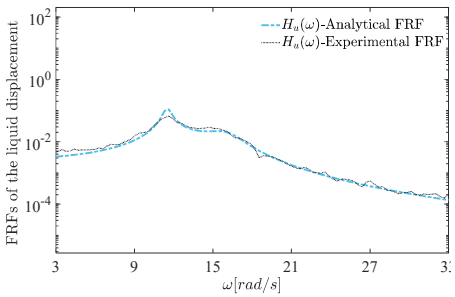

(a)

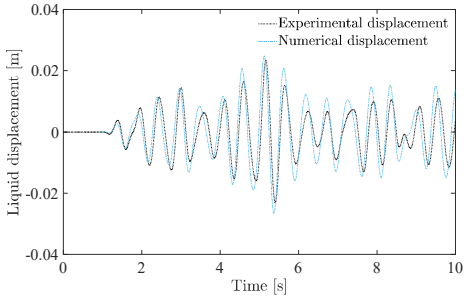

(b)

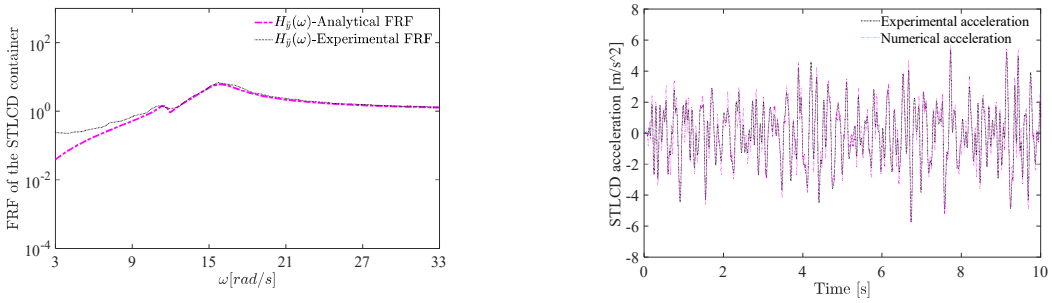

(c) (d)

Fig. 10 Response of the STLCD device in terms of (a) FRFs and (b) time history of the liquid displacement; (c) FRFs and (d) time history of the total acceleration of the STLCD container

5.3 Performance evaluation of the STLCD-controlled structure

Finally, the dynamic behavior of the controlled system equipped with the STLCD is studied. In particular, since the previous results have shown that the slightly nonlinear behavior of the STLCD device can be captured sufficiently accurately by linear analytical models, the equivalent linear equations for the STLCD-controlled structure were taken into account. The previously identified parameters of the various subsystems were incorporated into the analytical model, and numerical accelerations were derived and compared with the experimental data. Table 2 summarizes the results concerning of the identification procedures for each of the analyzed subsystems.

Table 2. Identified parameters

System	Frequency	Damping ratio
Main system	$\omega_s = 19.13$ rad/s	$\zeta_s = 0.0102$
STLCD	$\omega_2 = 15.49$ rad/s	$\zeta_2 = 0.079$
	$\omega_l = 11.74$ rad/s	$\zeta_l = 0.023$

Fig. 11 shows the responses of each degree of freedom of the STLCD-controlled structure under resonant conditions. Specifically, in Fig. 11 (a)-(b)-(c) the experimental STLCD acceleration, liquid displacement and roof total acceleration are plotted against the numerical ones. As can be observed, the equivalent linear mathematical model of the entire STLCD-controlled structure in Eq. (3), described by the parameters derived from the dynamic identification of each subsystem, can be considered reliable for predicting the real behavior of the small-scale model. This is evidenced by the close agreement between the experimental and numerical solutions. Interestingly, in Fig. 11 (a) the numerical acceleration underestimates the acceleration of the experimental response during positive acceleration peaks, while both responses are closely aligned at the negative peaks. In fact, the expected symmetrical response predicted by the numerical procedure, is not fully realized by the experimental model. This discrepancy may be attributed to a potential imperfection in the behavior of the spring connecting the STLCD device to the roof plate, which exhibits differing characteristics under compression and tension, particularly in conditions close to its resonance, possibly due to wear and tear associated with prolonged use.

In a final study, the performance control of the STLCD-controlled structure is experimentally evaluated against the benchmark uncontrolled SDOF structure, the SDOF structure equipped with the corresponding fixed TLCD (Fig. 12(b)), and the SDOF structure equipped with a traditional Tuned Mass Damper (TMD) (Fig.12c). The TMD was realized by using a solid mass with the same mass as the STLCD and mounted on the same sliding guide connected to the roof plate by the spring. Since the TLCD was not practically applicable to this type of structure, comparisons were made with a TLCD with the same STLCD mass ratio. Specifically, the different control strategies were tested under harmonic and sweep signal excitation.

The effect of the proposed control strategy on reducing the roof accelerations is depicted in Fig. 13 (a) under resonance conditions. It can be seen that the accelerations can be significantly mitigated by up to 70% when the STLCD is attached to the SDOF structure (red dash-dotted line). As expected, the untuned TLCD provides no

benefit to the structure. On the other hand, it is shown that, the STLCD has a clearly superior performance compared to the TLCD (blue dashed line) with the same mass while its performance is very similar to the TMD. (green line). These results are confirmed by the tests conducted by exciting the aforementioned small-scale models with a sweep signal and analyzing their response in the frequency domain. In this regard, Fig. 13(b) shows the response of the uncontrolled structure, the TLCD-controlled structure, the TMD-controlled structure, and the STLCD-controlled structure in terms of the FRF of the roof acceleration. As can be seen, the traditional TLCD shifts the fundamental frequency of the system without significantly suppressing the peak response. On the contrary, the STLCD results in a flatter FRF, suggesting that the STLCD device can be considered an attractive device for effectively reducing the accelerations of SDOF systems due to the versatility of its tuning procedure.

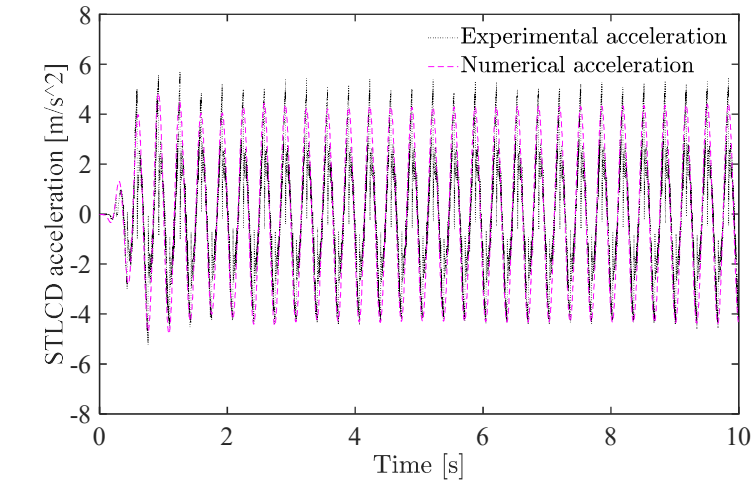

(a)

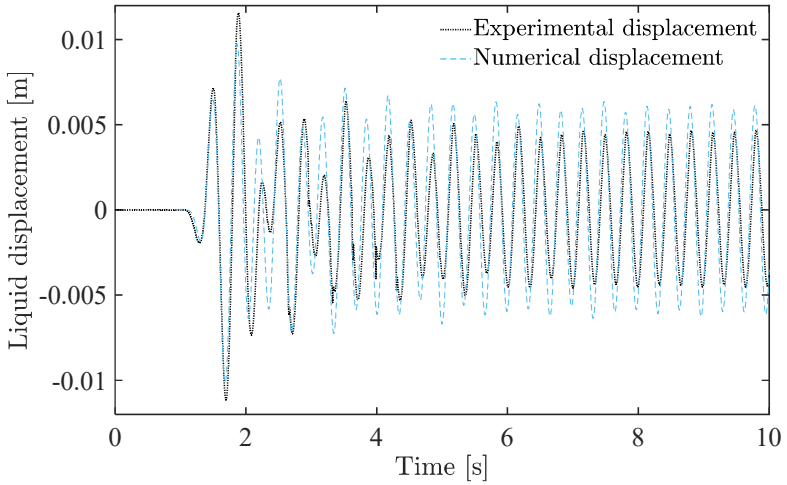

(b)

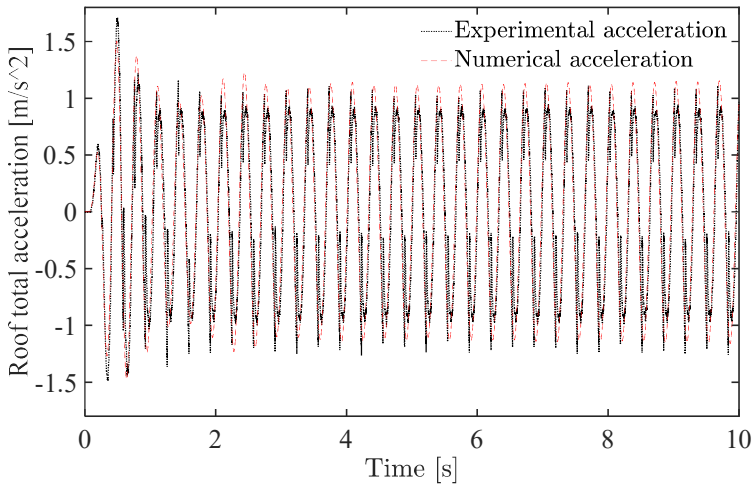

(c)

Fig. 11 Response of the STLCD-controlled structure in resonance conditions. (a) Acceleration of the STLCD container; (b) liquid displacement; (c) roof total acceleration

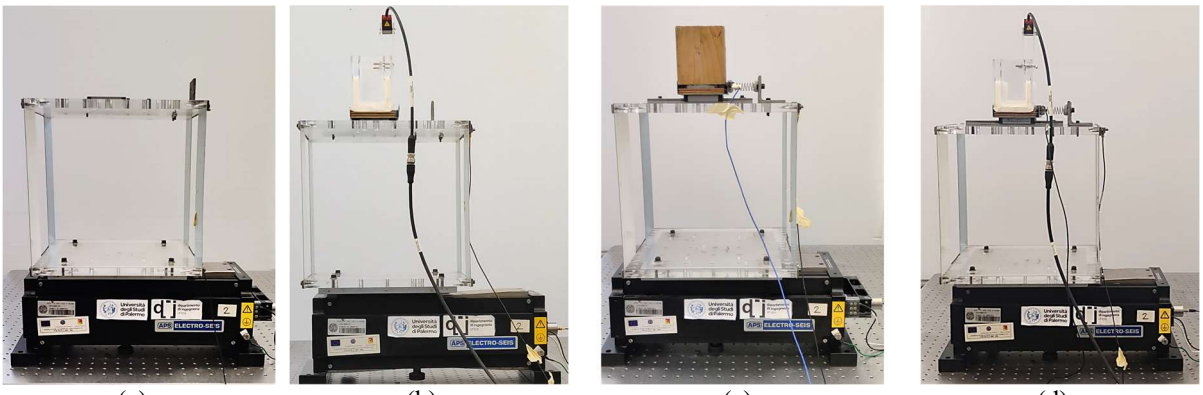

(a) (b) (c) (d)

Fig. 12 Small-scale models: (a) Uncontrolled structure; (b) TLCD-controlled structure; (c) TMD-controlled structure; (d) STLCD-controlled structure

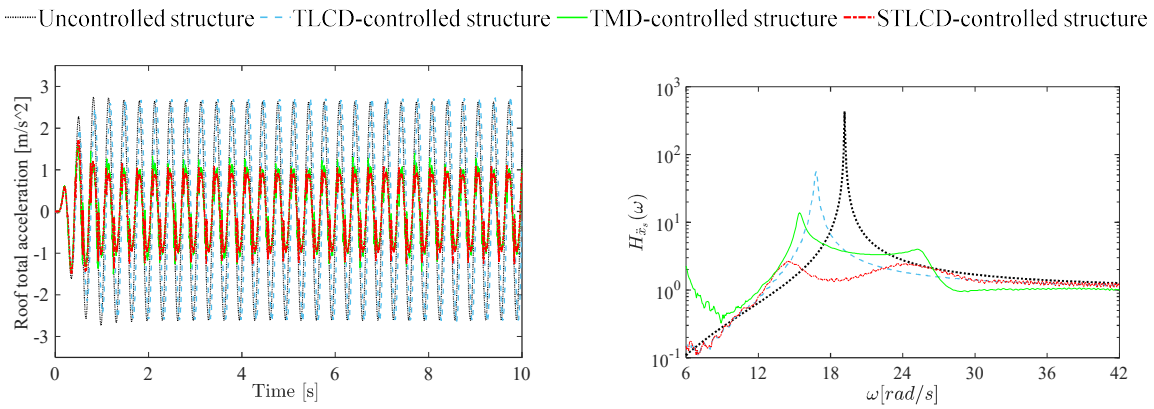

(a) (b)

Fig. 13 Response of the STLCD-controlled structure compared to the uncontrolled structure, the TLCD-controlled structure and TMD-controlled structure: (a) Roof total acceleration in resonance conditions, (b) FRF of the roof acceleration

6 Conclusions

In this study, a sliding version of the Tuned Liquid Column Damper (STLCD) was introduced as an alternative to the conventional TLCDs for mitigating seismic vibrations in short-period structures. Unlike TLCDs, the STLCD has the potential for broader applicability due to its improved tunability. Owing to the inherent nonlinearities, a complex numerical solution scheme is usually required to optimally design the device. Therefore, for design purposes, the nonlinear governing equations of motion of the STLCD-controlled structure are linearized through a statistical linearization technique and an optimization formulation for designing the STLCD, using explicit closed-form solutions, has been proposed. This is achieved by considering a Gaussian white noise model as the base excitation and minimizing the total acceleration variance of the equivalent linearized system. The validity of the proposed expressions is verified by comparison with results obtained from a more computationally intensive numerical iterative method. In addition, the efficiency of the optimized STLCD in reducing structural accelerations is investigated through experimental tests on a shake table. Specifically, a small-scale model of the STLCD-controlled structure was analyzed in comparison with the same structure controlled with traditional TLCD, Tuned Mass Damper (TMD) and with the uncontrolled structure. The results demonstrated that the slightly nonlinear behavior of the system can be accurately approximated by a linear analytical model. Moreover, the roof accelerations were reduced by up to 70% under sinusoidal harmonic ground acceleration. The experimental tests conducted on this scaled model highlight the effectiveness of the STLCD-based control strategy over the conventional approach involving TLCD as a seismic protection measure and emphasize the adaptability of STLCD devices to short-period structures in the field of structural control. Although the observed 70% reduction in roof accelerations is promising, further studies under realistic seismic conditions are essential. To extend the scope of this investigation, future research efforts will include testing different configurations of the STLCD device under recorded ground motions to evaluate the device efficacy in scenarios that closely mimic real-world seismic conditions.

Acknowledgement

C. Masnata and A. Pirrotta gratefully acknowledge the support received from the project SiciliAn MicronanOTecH Research And Innovation CEnter "SAMOTHRACE" (MUR, PNRR-M4C2, ECS_00000022), spoke 3 - Università degli Studi di Palermo "S2-COMMs - Micro and Nanotechnologies for Smart & Sustainable Communities.

References

1. Sakai, F., Takeda, S., Tamaki, T.: Tuned Liquid Column Damper - New Type Device for Suppression of Building Vibrations. In: Proceedings of the International Conference on Highrise Buildings, Nanjing, China, pp. 926–931 (1989).

2. Hochrainer, M.J., Ziegler, F.: Control of tall building vibrations by sealed tuned liquid column damper.

Structural Control and Health Monitoring 13 (6), 980–1002 (2006).

3. Fei, Z., Jinting, W., Feng, J., et al.: Control performance comparison between tuned liquid damper and tuned liquid column damper using real-time hybrid simulation. Earthquake Engineering and Engineering Vibration 18, 695–701 (2019).

4. Konar T., Ghosh A.: A review on various configurations of the passive tuned liquid damper. Journal of Vibration and Control 0(0), 1-36 (2022).

5. Park, ByungJin et al.: Vibration control of a structure by a tuned liquid column damper with embossments. Engineering Structures 168, 290-299 (2018).

6. P.A. Hitchcock, K.C.S. Kwok, R.D. Watkins: Characteristics of a liquid column vibration absorber (LCVA) - Part I. Engineering Structures, 19(2), 126-134 (1997).

7. T. Balendra, C.M. Wang, G. Rakesh: Vibration control of various types of buildings using Tuned Liquid Column Dampers (TLCD). Journal of Wind Engineering and Industrial Aerodynamics, 83, 197-208 (1999).

8. Balendra T., Wang, C., Cheong, H.: Effectiveness of tuned liquid column dampers for vibration control of towers. Engineering Structures 17(9), 668–75 (1995).

9. Ziegler, F.: The tuned liquid column damper as a cost-effective alternative for the mechanical damper in civil engineering structures. Journal of Acoustics and Vibrations 12, 25–39 (2007).

10. Sun, K.: Earthquake responses of buildings with liquid column dampers. Proceedings of the Fifth US National Conference on Earthquake Engineering, Chicago, Vol. II, 411–20 (1994).

11. Min KW, Kim HS, Lee SH, Kim H, Ahn SK: Performance evaluation of tuned liquid column dampers for response control of a 76-story benchmark building. Engineering Structures 27(7), 1101–1112 (2005).

12. Wu JC, Shih MH, Lin YY, and Shen YC: Design guidelines for tuned liquid column damper for structures responding to wind. Engineering Structures 27(13), 1893–1905 (2005).

13. Shum, K.M.: Closed form optimal solution of a tuned liquid column damper for suppressing harmonic vibration of structures. Eng. Struct. 31, 84–92 (2009).

14. Chang CC: Mass dampers and their optimal designs for building vibration control. Engineering Structures 21, 454–463 (1999).

15. A. Di Matteo, F. Lo Iacono, G. Navarra, A. Pirrotta: Direct evaluation of the equivalent linear damping for TLCD systems in random vibration for pre-design purposes. Int. J. Non Linear Mech. 63, 19–30 (2014).

16. A. Di Matteo, F. Lo Iacono, G. Navarra, A. Pirrotta: Optimal tuning of tuned liquid column damper systems in random vibration by means of an approximate formulation. Meccanica 50(3), 795–808 (2015).

17. Di Matteo A., Masnata C., Pirrotta A.: Hybrid passive control strategies for reducing the displacements at the base of seismic isolated structures. Frontiers in Built Environment 5, 2297-3362 (2019).

18. Di Matteo A., Furtmüller T., Adam C., Pirrotta A.: Optimal design of tuned liquid column dampers for seismic response control of base-isolated structures. Acta Mechanica 29, 437-54 (2018).

19. Furtmüller T., Di Matteo A., Adam C., Pirrotta A.: Base-isolated structure equipped with tuned liquid column damper: An experimental study. Mechanical Systems and Signal Processing 116, 816-831 (2019).

20. Adam C., Di Matteo A., Furtmüller T., Pirrotta A.: Earthquake excited base-isolated structures protected by tuned liquid column dampers: design approach and experimental verification. Procedia Engineering 199, 1574-79 (2017).

21. Ghosh A., Basu B.: Seismic vibration control of short period structures using the liquid column damper. Engineering Structures 26(13), 1905-13 (2004).

22. Roberts JB, Spanos PD: Random Vibration and Statistical Linearization. Chichester, 1990.

23. Di Matteo, A., Masnata, C. Adam, A. Pirrotta: Optimal Design of Tuned Liquid Column Damper Inerter for vibration control. Mechanical Systems and Signal Processing 167, 108553 (2022).

24. Masnata C., Di Matteo A., Adam C., Pirrotta A.: Efficient estimation of tuned liquid column damper inerter (TLCDI) parameters for seismic control of base-isolated structures. Computer-Aided Civil and Infrastructure Engineering 00, 1-19 (2022).

25. D. De Domenico, G. Ricciardi: An enhanced base isolation system equipped with optimal tuned mass damper inerter (TMDI). Earthq. Eng. Struct. Dyn. 47, 1169–1192 (2018).

26. Di Paola M., Elishakoff I.: Non-stationary response of linear systems under stochastic Gaussian and non-Gaussian excitation: a brief overview of recent results. Chaos, Solitons & Fractals, Volume 7, Issue 7, 961-971 (1996).

27. Zhao Z., Zhang R., Jiang Y., Pan C.: A tuned liquid inerter system for vibration control. Int. J. Mech. Sci. 164, 105171 (2019).

28. Perez R.E., Behdinan K.: Particle swarm approach for structural design optimization. Comput. Struct. 85(19):1579-1588 (2007).

29. Gutierrez Soto, M. and Adeli, H.: Recent Advances in Control Algorithms for Smart Structures and Machines. Expert Systems 34(2), 14 pages, e12205 (2017).

30. J.P. Den Hartog, Mechanical Vibrations, New York, McGraw-Hil, NY, 1956.

31. Håvard V., Crowley J. and Rocklin G.T.: New Approaches to Frequency Response Function Estimation. Sound and Vibration 18, pp. 34-38 (1984).

32. Levenberg K: A Method for the Solution of Certain Problems in Least-Squares. Quarterly Applied Mathematics 2, 164-68 (1944).

33. Shampine, L. F. and M. W. Reichelt, “The MATLAB ODE Suite,” SIAM Journal on Scientific Computing, Vol. 18, 1997, pp. 1–22.